

Census-block-level Property Risk Assessment for Wildfire in Louisiana, U.S.A.

Rubayet Bin Mostafiz^{1*}, Carol J. Friedland², Robert V. Rohli¹, Nazla Bushra¹

¹Department of Oceanography & Coastal Sciences, College of the Coast & Environment, Louisiana State University, Baton Rouge, LA 70803

²Bert S. Turner Department of Construction Management, College of Engineering, Louisiana State University, Baton Rouge, LA 70803

*** Correspondence:**

Rubayet Bin Mostafiz
rbinmo1@lsu.edu

Keywords: Wildfire, Natural hazards, Population projections, Forest resources, Vulnerability, Resilience, Environmental change, Climate change

Abstract

Wildfire is an important but understudied natural hazard. Research on wildfire, as with other natural hazards, is all too often conducted at a spatial scale that is too broad to identify local or even regional patterns. This study addresses these research gaps by examining the current and future wildfire risk, considering projections of population and property value, at the census-block level in Louisiana, a U.S. state with relatively dense population and abundant timber resources that would be vulnerable to loss from this hazard. Here wildfire risk is defined as the product of vulnerability to the hazard (which is itself defined as the product of burn probability, damage probability, and percent damaged) and exposure to the hazard, the latter of which is represented here by property value. Historical data (1992–2015) suggest that the highest risk is in southwestern inland, east-central, extreme northwestern, and coastal southwestern Louisiana. Based on existing climate and environmental model output, this research assumes that wildfire will increase by 25 percent by 2050 in Louisiana from current values. When combined with projections of population and property value, it is determined that the geographic distribution of risk by 2050 will remain similar to that today – with highest risk in southwestern inland Louisiana and east-central Louisiana. However, the magnitude of risk will increase across the state, especially in those areas. These results will assist environmental planners in preparing for and mitigating a substantial hazard that often goes underestimated.

INTRODUCTION

Although weather-related disasters cause extensive and rapidly increasing damage worldwide, efforts to understand the holistic risk from these hazards are still in progress. While a growing amount of research is focusing on assessing risk due to flood, hurricane, tornado, and extreme weather events, the wildfire risk is lesser-studied and often limited to the regions that are more susceptible to extreme economic loss. Because wildfire is a critical ecosystem process influenced by a combination of natural and human factors (Lasslop and Kloster 2017), and because its presence and intensity can be modified by climate change (Piñol et al. 1998; Malamud et al. 2005; Mokhov et al. 2006; Cannon and DeGraff 2009; Flannigan et al. 2009; Marlon et al. 2009; Moritz 2012; Enright and Fontaine 2014) it must be considered in environmental risk assessment. Most of the existing wildfire research in the U.S.A. focuses on the West, as it is the major wildfire vulnerability area (Cannon and DeGraff 2009; Ager et al. 2013; Dennison et al. 2014; Holden et al. 2018; Ager et al. 2021). The historical record shows that the western U.S.A. has generally experienced increasing wildfire frequency and intensity over time (Running 2006; Westerling et al. 2006; Dennison et al. 2014; Higuera et al. 2015; Abatzoglou and Williams 2016; Westerling 2016; Holden et al. 2018). Despite earlier research that suggested that wildfire occurrence in Mississippi had decreased since the 1920s (Grala and Cooke 2010), the volume of wildfire risk-related research on the U.S. Southeast deserves more attention, especially because of the droughts in recent years (Schubert et al. 2021), dense population, and high probability of risk from other wildfire-related hazards. Louisiana is particularly understudied regarding wildfire.

The impacts of wildfire are three-fold: environmental, health, and property. In recent decades, environmental research has emphasized the importance of studying wildfire dynamism, variability, and the factors affecting them at the regional level (Morgan et al. 2001; Vázquez et al. 2002; Cleland et al. 2004; De la Riva et al. 2004; Schoennagel et al. 2004; Malamud et al. 2005; Moreira et al. 2009; de Zea Bermudez et al. 2010; Aldersley et al. 2011; Strydom and Savage 2017; Colantoni et al. 2020), in part because climate change implications on ecosystems (Davis et al. 2019) present unique challenges for hazard management in each wildfire-regime. Regarding human health impacts, Louisiana has been found, along with Florida and Georgia, to be most affected by hospital admissions and premature deaths due to wildfire events in the U.S.A. (Fann et al. 2018), in addition to generally unhealthy conditions due to wildfire-related smoke (Kaulfus et al. 2017; Sorensen et al. 2021). Fann et al. (2018) showed a map that suggests that PM_{2.5} concentrations in Louisiana attributed to wildfire exceeded that of any other state except California in 2008. From a property loss perspective, wildfire impacts have been substantial, especially at the wildland–urban interface (WUI; Radeloff et al. 2005) – the area where development meets wildland vegetation. In a holistic cost/benefit or “hedonic” approach, Hansen et al. (2014) found a negative effect of wildfire on property values in California, Colorado, and Montana, with less conclusive evidence from research based elsewhere in Colorado and in Alaska. Further work showed that home prices and sales rates in the Front Range of Colorado are influenced by wildfire risk and risk perceptions (McCoy and Walsh 2018). Other research has examined the impacts of wildfire risk on residential property values in the Netherlands (Magnée 2020). Property damage in northeastern Florida due to wildfires in the El Niño year of 1998 was estimated at \$10–12 million (Butry et al. 2001). And more recently, programs like FireSmart (Ergibi and Hessel 2020) provide homeowners in the WUI with information to make more informed decisions for protecting their property from the wildfire

hazard. However, few if any Louisiana-based studies exist on the topic of wildfire and property losses.

This paper presents a census-block-level property risk assessment for wildfire in Louisiana, U.S.A. Community level wildfire risk analysis is necessary to improve wildfire mitigation planning (Ager et al. 2015). The three primary objectives are to: 1) characterize the historical wildfire burn probability; 2) project the future wildfire burn probability; and 3) assess the future property loss in Louisiana due to wildfire, considering anticipated changes to climate and population. Integration of natural and social science approaches as shown in the three objectives here are needed to understand more fully the risk of wildfire, especially in light of climate change concerns (Ayres et al. 2016). The results will benefit foresters, property owners, and mitigation specialists within and beyond Louisiana as they seek new and improved ways to characterize and prepare for the wildfire hazard.

BACKGROUND

A wildfire is combustion in a natural setting, marked by flames or intense heat, ranging in coverage from less than 20 hectares to over 3 million hectares. Over the period from 2007 to 2016, an annual average of 1,431 wildfires burned 14,950 acres of forestland in Louisiana, with most of these fires caused by arson or carelessness/negligence committed by people, exacerbated by human confrontation with nature (Louisiana Department of Agriculture & Forestry (LDAF) 2021). Likewise, lightning was found to be a minor cause of wildfire in Mississippi compared to anthropogenic causes (Grala and Cooke 2010). Using the customary categorization of U.S. wildfires as large (> 300 acres) or small (< 300 acres), Louisiana wildfires tend to be small, averaging about 10 acres in size (LDAF 2021). At the WUI, both vegetation and the built environment provide fuel for fires. Wildfire does not include prescribed burns (Penman et al. 2020) or fires started in a building.

Natural and human-prescribed fire is often healthy (Hamilton and Salerno 2020; Hood et al. 2020). Fire restores nutrients to the soil and provides new niches while often leaving native species unharmed or resilient to the disturbance, in general (Binkley et al. 2007) as well as in Louisiana (Jones and Chamberlain 2004; Haywood 2011; Simmons and Bossart 2020). In addition, fire is also useful at combatting pests, diseases, and fungal growth, allowing for the post-fire regrowth to establish hardier individuals. Frequent fire return intervals have been found to be effective means of maintaining ecosystems in Louisiana (Haywood et al. 2000; Drewa et al. 2002; Stambaugh et al. 2011; Yeldell et al. 2017).

Wildfire can also be a substantial hazard, including in Louisiana. As development near the WUI continues, more natural ecosystems, people, and property are exposed to wildfire danger (Theobald and Romme 2007). Aside from the obvious impacts of habitat destruction and potential loss of food supply, documented impacts of wildfires to ecosystems in Louisiana include weakened ecosystem resilience in salt marshes (Jones et al. 2020).

The Keetch-Byram Drought Index (KBDI; Pharo and Croom 1971), which is calculated based on observed or simulated changes in maximum temperature and precipitation, has been used frequently to assess wildfire vulnerability (e.g., Liu et al. 2009; Gannon and Steinberg 2021). The KBDI is scaled to suggest the number of millimeters of precipitation that would be required

to saturate the soil (i.e., reduce the KBDI to zero). Values from 0 to 200 indicate minimal wildfire threat, with values of 200 to 400 suggesting that the lower litter layer is drying and beginning to be susceptible to drought. Values from 400 to 600, which are more typical of late summer and early autumn, indicate a moderate burn potential. Values of 600 to 800 are associated with more severe drought and active potential for burning.

Several studies have evaluated wildfire probability with the goal of anticipating future losses, understanding migration and adaptive capacities, and avoiding losses due to increased frequency and intensity. Li et al. (2009) used an artificial neural network approach for modeling the impact of population density and weather parameters such as average relative humidity, wind velocity, and daily sunshine hours to forest fire risk in Japan. Thompson et al. (2013) introduced a polygon-based spatially explicit burn probability model to assess exposure of resources and assets to wildfire. Incorporating both natural and anthropogenic ignitions, Ager et al. (2013) proposed a wildfire simulation model which characterizes potential wildfire behavior in terms of annual burn probability and flame length by analyzing a set of social and ecological parameters in the Oregon and Washington national forests. Ager et al. (2014) examined the spatiotemporal patterns of the wildfire occurrence in Sardinia, Italy, and characterized the outcomes of both the probability of ignition and large fire in terms of weather, land use, anthropogenic features, and time of year. Based on wildfire likelihood and intensity over the 1992 to 2010 period, Dillon et al. (2015) developed a broad-scale wildfire potential map for the contiguous U.S.A. that can be used to analyze wildfire threat or risk to structures or power lines. To assess wildfire risk probability, Short et al. (2016) created national burn probability (BP) and conditional fire intensity level (FIL) estimates at a 270-m grid resolution over the contiguous U.S. using the U.S. Forest Service Missoula Fire Sciences Laboratory's geospatial Fire Simulation system (FSim), which includes scenarios for generating wildfire-conducive weather, wildfire occurrence, fire growth, and fire suppression. Based on the minimum travel time algorithm, Alcasena et al. (2016) developed a fire simulation model to analyze the wildfire exposure of highly valued resources and assets in a 28,000 ha area in central Navarra, Spain. Bui et al. (2017) generated a GIS-based novel hybrid artificial intelligence approach to model spatial susceptibility of the wildfire hazard in the central highland forest region of Vietnam. Papakosta et al. (2017) built a probabilistic model for predicting wildfire housing loss at the mesoscale (1 km²) level using Bayesian network analysis, enabling the construction of an integrated model based on causal relationships among the influencing parameters jointly with the associated uncertainties. Hong et al. (2019) predicted the spatial pattern of wildfire susceptibility in Huichang County, China, by using the integrated probabilistic "weights-of-evidence" and knowledge-based "analytical hierarchy process" models. Jaafari et al. (2019a) developed a wildfire prediction model incorporating ten geophysical and climatological parameters to investigate the spatial distributions of wildfire probabilities from 32 fire events at the Zagros ecoregion of Iran. In recent years, use of rigorous data interpretation techniques such as geographical information systems (GIS), and statistical and machine learning approaches have resulted in various prediction models of wildfire probability (Preisler et al. 2004; Catry et al. 2010; Bui et al. 2017; Tutmez et al. 2018; Jaafari et al. 2018, 2019a, 2019b; Hong et al. 2019). This paper will be the first to project the future property loss at micro-scale (census block level) in Louisiana considering the historical wildfire occurrence and damage data, climate, and population change.

STUDY AREA

Louisiana is selected as the focus of this research for several reasons. First, the state lies in an area that, despite abundant rainfall, can be subjected to periods of drought (Bushra et al. 2019) and therefore wildfire. These wildfires can have disproportionate impacts because of the heavy reliance of wet-environment land uses, such as rice farming, industrial applications, and recreation. Second, as will be shown later in this manuscript, these periods of wildfire are expected to increase in frequency in the future in Louisiana as in much of the rest of the United States. Third, the state is relatively densely populated, particularly compared to most of the wildfire-vulnerable Western U.S., causing anthropogenic activity to contribute substantially to the hazard and human impacts of the hazard to be intensified. And fourth, in recent years Louisiana has ranked first among U.S. states in acreage harvested for short rotation woody crops in the last two agricultural censuses in 2012 and 2017 (United States Census of Agriculture 2017, Table 36, p. 617), making it vulnerable to economic loss due to wildfire.

DATA

Because wildfire outside but near Louisiana can endanger the state, a 50-km buffer to include adjacent Texas, Arkansas, and Mississippi is analyzed along with Louisiana. To address the first objective – characterizing the historical wildfire probability – historical wildfire occurrence data from 1992 to 2015 from Short (2017) and large wildfire burn probability from Short et al. (2020) are used. The second objective – projecting the future wildfire probability – relies on information from the fourth National Climate Assessment (U.S. Global Change Research Program (USGCRP) 2017). USGCRP (2017) follows the method of the Intergovernmental Panel on Climate Change (IPCC) by running fossil fuel emission scenarios termed “representative concentration pathways” (RCPs), with the scenarios numbered based on the amount of radiative forcing (in W m^{-2}) anticipated in the year 2100, such that RCP8.5 is the most severe scenario. As in the vast majority of contemporary climate change-based research, the model results using the RCPs are based on the Climate Model Intercomparison Project (CMIP). Results from IPCC’s fifth assessment report are available in USGCRP (2017). Other scenarios account for changes in economic growth, environmental values, globalization, and regionalization.

To address the objective of assessing the future property loss in Louisiana due to wildfire considering anticipated changes to climate and population, Louisiana census-block shapefiles are downloaded from the U.S. Census Bureau (2010). Likewise, population projections are based on data from U.S. Census Bureau (2021). LDAF detailed fire summary data for Louisiana (2007–2017; Bret Lane, personal communication, 4/9/2018) serve as a baseline for future property loss due to wildfire.

METHODOLOGY

Method for Assessing Historical Wildfire Burn Probability

A method of computing both large and small fire probabilities is necessary here because FSim focuses on large (> 300 acres) fires (Dillon et al. 2015) and fires in and near Louisiana are primarily classified as “small.” The wildfire probability calculation follows the method of Dillon et al. (2015), which uses large fire (i.e., > 300 acres) probability from FSim (Finney et al. 2011)

supplemented by a collection of small fire (i.e., < 300 acres) probabilities from the Fire Protection Agency (FPA) fire occurrence data (Short 2013). The total probability is calculated as the sum of large and small fire probability.

Large wildfire burn probability raster files are downloaded from U.S. Department of Agriculture (Short et al. 2020). Then, the “Extract by Mask” tool in ArcGIS® is used to delineate the study area, yielding the large fire probabilities for the study area. To extract the small fire probabilities, the nationwide fire occurrence point-based shapefiles (1992–2015) from U.S. Department of Agriculture (Short 2017) are downloaded, and fires larger than 300 acres are removed. Small wildfire occurrence are then extracted for Louisiana and surroundings using the “clip” tool in ArcGIS. A total of 73,501 small fire records exist in Louisiana and within the 50-km buffer. Planar kernel density analysis (Silverman 1986) is then performed for the small fire data, to produce a spatial distribution of fire density, with cell size set to 270 m, to correspond to that used in the FSim layer, and a kernel size of 50 km (Dillon et al. 2015). The cell area ($270\text{m} \times 270\text{m} = 72,900 \text{ m}^2$) is then multiplied by the resulting kernel density of fire. To identify the small fire probability over the smoothed surface, the total number of fires (73,501) is divided by the kernel density, and this value for each pixel is divided by 24 to compute the historical (1992–2015) annual probability. To calculate total fire annual probability, this small fire probability is added to the large fire probability from FSim. The 50-km buffer is then removed by masking with the Louisiana boundary. Finally, the wildfire burn probability of each census block $p(f)_i$ is extracted from the raster files at the centroid of each census block.

Method for Assessing Future Wildfire Burn Probability

The first step in determining future wildfire burn probability is to quantify the wildfire hazard based on model projections. USGCRP (2017) suggests an increase in lightning-ignited wildfire by 2050 in the U.S. Southeast, including Louisiana (Wehner et al. 2017). However, Wehner et al. (2017) reports that substantial intra-regional differences in wildfire vulnerability are likely to exist between ecoregions, and other research acknowledges the complicated interplay between modeled trends in individual variables that may have compensating effects in their influence on future wildfire intensity and probability.

This projected increase in wildfire vulnerability comes despite several possible mitigating factors. Anticipated water scarcity in a changing climate and intensifying insect infestations in a warming world may mitigate the wildfire hazard by reducing fuel from trees that are stunted by water scarcity or killed by insect infestations (Prestemon et al. 2016; Wehner et al. 2017), such as the southern pine beetle in Louisiana (Coleman et al. 2008). Other factors that might at first glance seem to mitigate future wildfire occurrence actually exacerbate the wildfire hazard. For example, daily precipitation totals are projected to increase by 9–13 percent for Louisiana by 2050, amid a generally more extreme precipitation climate nationwide by 2100 (Wehner et al. 2017). But this enhanced “per event” precipitation and sharp increase in the frequency of days having a greater than 90th percentile of precipitation are accompanied by substantially more frequent “zero precipitation days” and small precipitation totals that would fall within today’s zero-to-tenth-percentile (Wehner et al. 2017). The warmer atmosphere is projected to support more moisture before saturation is reached, but future tropical precipitation extremes are not simulated reliably and changes in extratropical precipitation extremes are dampened compared with the increases atmospheric water vapor content (e.g., O’Gorman and Schneider 2009).

Furthermore, the anticipated weakening of steering circulation (Vautard and Yiou 2009) that moves frontal and tropical weather systems will leave longer interarrival times between intense precipitation events. These factors contribute to the anticipated increase in wildfire in Louisiana and elsewhere, as longer runs of dry days are expected.

Obviously, such changes in both precipitation intensity and interarrival times would induce changes in soil moisture, which in turn would change wildfire burn probability. Wehner et al. (2017) acknowledge that projections of seasonal precipitation deficits lack confidence, but they recognize that the preponderance of evidence suggests that enhanced evapotranspiration caused by increased temperatures will outpace the projected increasing precipitation totals. The result is likely to be soil desiccation through this century over much of the continental U.S., including Louisiana, at least under the RCP8.5 scenario. The net impact of these changes for Louisiana is expected to be small soil moisture decreases in autumn relative to natural variability, but large decreases relative to natural variability in the other three seasons (Wehner et al. 2017). These soil moisture forecasts are made with a “medium” degree of confidence, supporting the notion that wildfire intensity will increase by mid-century. Such results are corroborated by Prestemon et al. (2016), who used three general circulation models and three IPCC-based emission scenarios to conclude that median annual area of the U.S. Southeast affected by lightning-ignited wildfire will increase by 34 percent, human-ignited wildfires will decrease by 6 percent, and total wildfire will increase by 4 percent by 2056–60 compared with the years 2016–2020.

Liu et al. (2009) modeled seasonal changes to the KBDI using the A2a economic/environmental/globalization/regionalization scenario, which assumes that global population surpasses 10 billion by 2050, with relatively slow economic and technological development, creating global CO₂ mixing ratios of 575 parts per million (ppm) by 2050 and 870 ppm by 2100 (compared to the current 418 ppm). Validation of output from four general circulation models for global climate for the 1961–1990 period led Liu et al. (2009) to conclude that the Hadley Centre climate model version 3 (Pope et al. 2000) is most effective for simulating global KBDI for the 2070–2100 period. In autumn and winter (September through February), decreases of 50–150 mm per three-month period were forecasted in Louisiana, while in March through May and June through August, decreases of 200–250 mm per three-month period were projected in Louisiana (Liu et al. 2009, their Figure 5).

The midpoint of the time series of the projection by Liu et al. (2009) is 2085, so the current research assumes that half of the projected changes in KBDI will occur by 2050. Thus, decreases of 25–75 mm per three-month period (or 8–25 mm per month, with 17 mm per month as the midpoint) are projected for each month from September through February in Louisiana by 2050. Decreases of 100–125 mm per three-month period (or 33–42 mm per month, with 38 mm per month as the midpoint) are projected for each month from March through August in Louisiana by 2050. Recent research (Krueger et al. 2017) suggests that the fraction of available water (FAW) is a better predictor of large growing-season wildfires than the KBDI. FAW is calculated as the ratio of plant available water to soil water capacity. But FAW has not yet been projected as confidently to 2050 as precipitation.

To provide more detail for Louisiana based on Liu et al.’s (2009) results, average monthly precipitation data for 31°N, 91.5°W (the nearest available data point to the center of the Louisiana state) are input into the Web-based, Water-Budget, Interactive, Modeling Program

(Willmott et al. 1985; WebWIMP 2021). Results suggest that decreases in soil moisture in the upper-layers of 12.2 percent (February) to 46.1 percent (August) are projected. Thus, a 25 percent decrease in available moisture in the organic matter and uppermost soil layers, and a 25 percent increase in wildfire susceptibility across Louisiana by 2050 ($F_{2050} = 1.25$) is projected here. These projections are not without their caveats. For example, these changes do not take into account projected changes in global air temperature. According to Frankson et al. (2017), despite the fact that little surface temperature warming occurred in Louisiana over the 20th century, historically unprecedented warming is to be expected, under a higher emissions pathway, by 2100.

Method of Projecting Population

The method of projecting population (P) at the census-block (i) scale by the year 2050 follows that of Mostafiz et al. (2020). Because annual census-block level population estimates are unavailable, the process begins with parish-wide annual growth rate calculations. For each parish (j), the average of the annual population growth rate (r_j) for the n -year (i.e., 40) period for which available annual U.S. Census Bureau estimates exist (i.e., 1980–2020) is calculated, beginning in year y , as described by Equation 1:

$$r_j = \frac{\sum_y^{y+n} \left[\frac{(P_{j,y+1} - P_{j,y})}{P_{j,y}} \right]}{n} \quad (1)$$

After r_j is determined for each of Louisiana's 64 parishes, future population change is downscaled to the census block (i), assuming that r_j is the same for each census block in its parish. Future population is then projected for each census block, assuming that currently unpopulated census blocks remain uninhabited through 2050. For each i , the 2010 population is used as the initial base (i.e., $P_{0,i} = P_{2010,i}$) and future population is projected out to 2050 (i.e., $P_{f,i} = P_{2050,i}$), given a n -year period within which the population changes (t), as shown in Equation 2:

$$P_{f,i} = P_{0,i} e^{r_j t} \quad (2)$$

This approach outperforms other methods that were tested. Specifically, the extension of a trend line of parish-level population into the future proved impractical because several parishes show an insignificant trend line and low explained variance. A second methodology tested is the extension of the growth rate trend line to approximate the 2050 population, but this proved problematic for the same reason. The abrupt, sizeable, and temporary population redistributions both within and beyond Louisiana resulting from significant hurricanes (most notably Katrina in 2005) are likely contributors to the low explained variance. The technique selected is least sensitive to these issues.

Method of Assessing Building/Structure Value

To address the third objective, it is necessary to evaluate current and future building/structure value in each census block. The total number of buildings in each census block in 2010 ($N_{2010,i}$) is computed from the U.S. Census Bureau (2010) by summing the buildings constructed during each time interval as reported in the shapefiles. Then this value is multiplied by the mean building value in 2010 in a given census block ($MV_{2010,i}$) to give the total inventory value in that census block ($I_{2010,i}$), as shown in Equation 3:

$$I_{2010,i} = N_{2010,i} \times MV_{2010,i} \quad (3)$$

The number of buildings in 2050 in a census block ($N_{2050,i}$) is assumed to change proportionately to population, so the population projection described above is used to scale the building inventory. Total inventory value in 2050 in a census block ($I_{2050,i}$) is then calculated as the product of total building inventory value in 2010 in that census block and the ratio of 2050 population to 2010 population.

$$I_{2050,i} = I_{2010,i} \times \frac{P_{2050,i}}{P_{2010,i}} \quad (4)$$

Method of Projecting Future Property Loss

Because LDAF records show that from 2007 to 2017, 389 of the 12,979 Louisiana residences that were threatened by fire were damaged (Bret Lane, personal communication, 4/9/2018), a conditional probability of damage $p(d|f_i)$ of 0.03 is assumed. In other words, three percent of buildings exposed to fire are damaged. Then, the probability of damage $p(d)_i$ is calculated as shown in Equation 5:

$$p(d)_i = p(f)_i \times p(d|f_i) \quad (5)$$

Based on LDAF advice, each damaged building is assumed to have a loss of 5 percent of the building value (Bret Lane, personal communication, 4/9/2018); thus, d is 0.05. Future property loss due to wildfire (L) in census block i is calculated as shown in Equation 6:

$$L_{2050,i} = I_{2050,i} \times p(d)_i \times d \times F_{2050,i} \quad (6)$$

All losses are expressed in \$2010. Similarly, the historical annual property loss $L_{1992-2015,i}$ is calculated using the 2010 building inventory at each census block $I_{2010,i}$, the probability of damage $p(d)_i$, and percent of damage, d . Annual per capita and per building property loss in 2010 and 2050 by census block are calculated by dividing by the population and building count, respectively.

RESULTS

Historical Wildfire Probability

Historical (1992–2015) wildfire burn probability ranges from 0 in coastal southeastern census blocks to 7.7 percent at a point in Cameron Parish (Appendix A), in the extreme coastal southwest (Figure 1A). The west-central, east-central, and extreme northwestern and southwestern parts of the state have the highest burn probability for wildfire (Figure 1A). Because planning is done at the parish level, it is also worthwhile to note that Washington (in extreme east-central Louisiana) is the most vulnerable parish, where the mean historical wildfire burn probability is 4.1 percent (Appendix A).

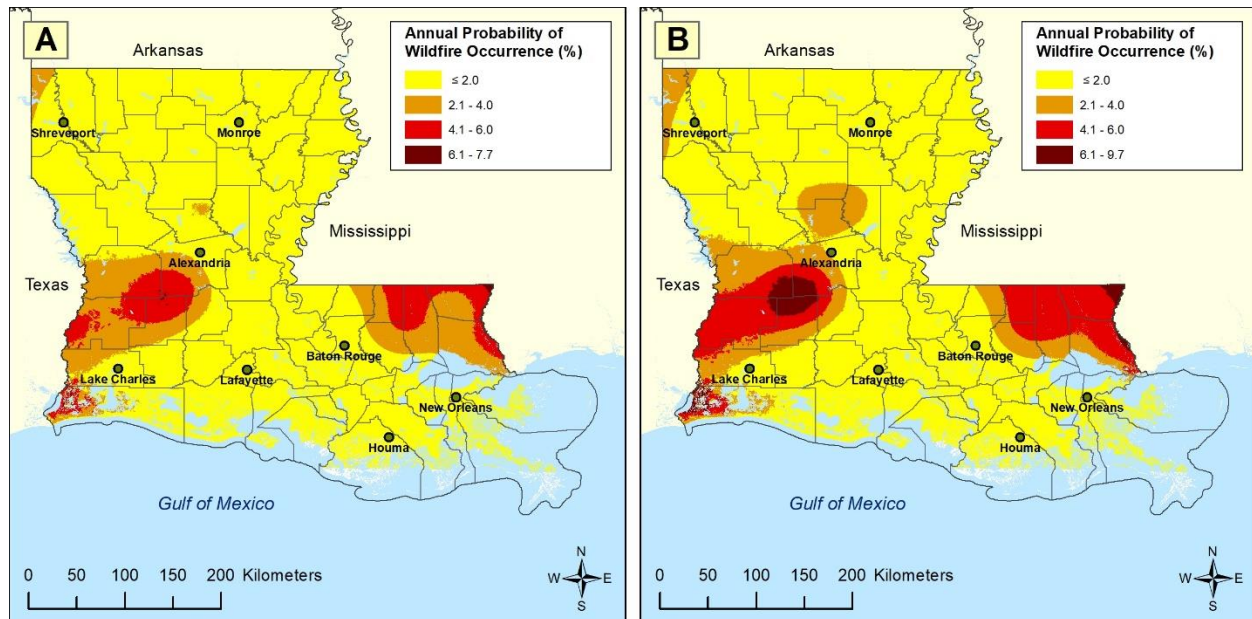


Figure 1 | Wildfire burn probability: (A) historical (1992–2015), and (B) projection for 2050.

Projected Future Wildfire Probability

By 2050 projected wildfire burn probability is anticipated to range from 0 on the southeast coast to 9.6 percent at a point in Cameron Parish (Figure 1B; Appendix B). The highest wildfire burn probability among census block centroids is expected to be 8.6 percent in census block 221179501012000 in Washington Parish. Washington will be the most vulnerable parish, where the mean projected wildfire burn probability is 5.2 percent (Appendix B). Washington, St. Helena, Beauregard, Allen, Tangipahoa, St. Tammany, Vernon, Rapides, Livingston, and Calcasieu are the top ten most vulnerable parishes in Louisiana (Appendix A-B), whereas St. Mary, Iberia, Terrebonne, Assumption, and Lafourche are the least vulnerable parishes (Appendix A-B). The wildfire hazard is likely to remain concentrated in the same geographical areas of the state as in the historical record, but burn probabilities are likely to increase (Figure 1A-B).

Projected Future Population

Using the values calculated in Equations 1 and 2, and assuming that the 102,781 census blocks (from among the 203,447 total) in Louisiana that were inhabited in 2010 will remain the only blocks inhabited in 2050, the 2050 population density projection is generated. Population is most densely concentrated around New Orleans, Baton Rouge, and Shreveport, the state's three largest cities (Figure 2A). By 2050, the population will remain concentrated in largely the same areas, but with increasing density around Lafayette, Baton Rouge, and in east-central Louisiana (Figure 2B). Population declines are expected throughout northeastern Louisiana east of Monroe, along the Red River Valley from Shreveport to the area southeast of Alexandria, in the New Orleans area, and elsewhere (Figure 2B). Appendix C shows these values by parish.

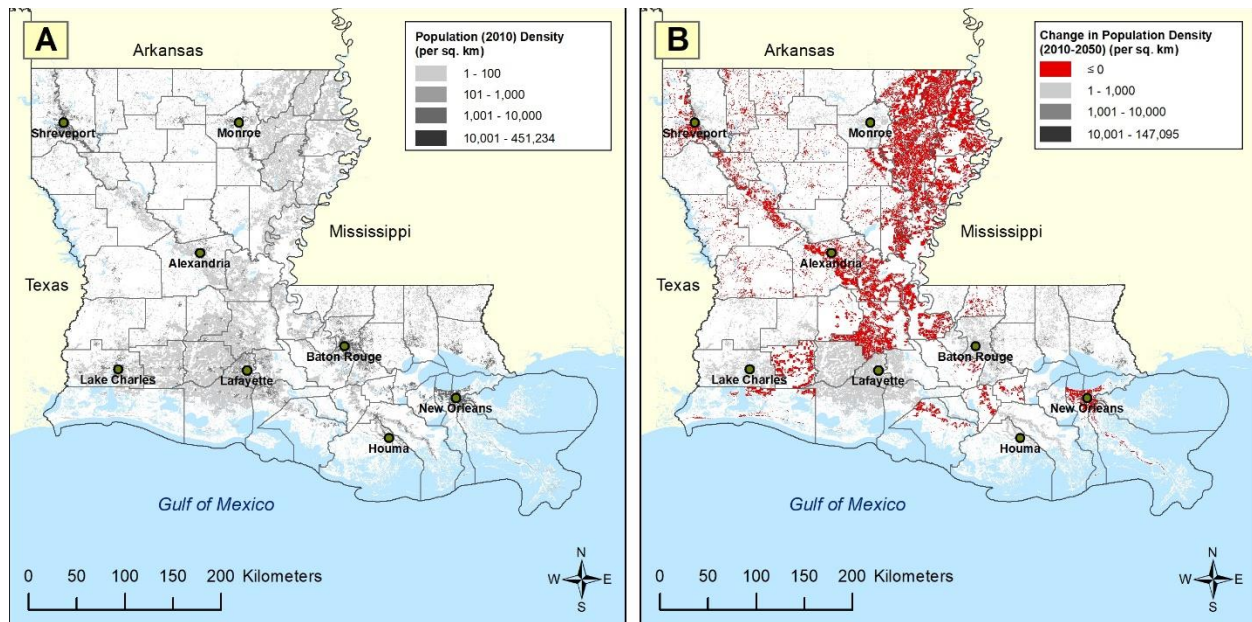


Figure 2| Population density by census block: (A) 2010, and (B) change in population density from 2010 to 2050.

Historical and Projected Future Property Loss

At the statewide level, the expanding WUI will increase the wildfire risk by 2050 as population and development, and therefore annual property loss due to wildfire, increase. The historical (1992–2015) average annual statewide property loss due to wildfire was \$3,169,064 (2010\$). Projected loss will be \$6,373,907 by 2050 (2010\$) due to the population growth, WUI, and climate change (Appendix D). Thus, the wildfire annual loss is projected to increase by 101 percent. The maximum estimated property losses will remain concentrated near their present locations, namely east-central, southwestern, and northwestern Louisiana (Figure 3A-B). On a per capita basis, the historical (1992–2015) average annual per capita property loss due to wildfire was \$0.70 (2010\$) in Louisiana (Appendix D). Projected per capita property loss is \$1.25 by 2050 (2010\$), giving an increase in annual per capita property loss of 61 percent (Appendix D). The same general spatial distribution of per capita property losses (Figure 4A-B) occurs (and is projected to occur by 2050) as was shown for absolute losses. The historical

average annual per building property loss was \$1.61 (2010\$) whereas the projected loss will be \$2.65 (2010\$) by 2050 (Appendix D). Thus, the annual per building property loss will increase by 64 percent in Louisiana. Again, the spatial distribution remains similar (Figure 5A-B).

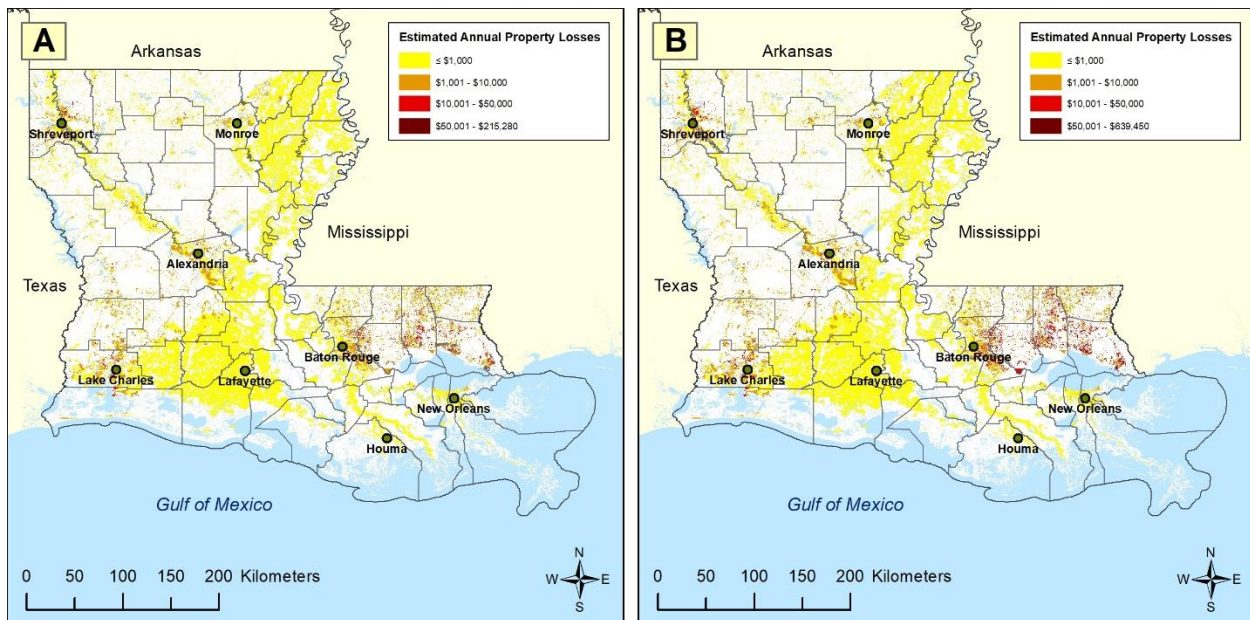


Figure 3| Estimated annual property loss (\$2010) due to wildfire by census block: (A) historical (1992–2015), and (B) 2050.

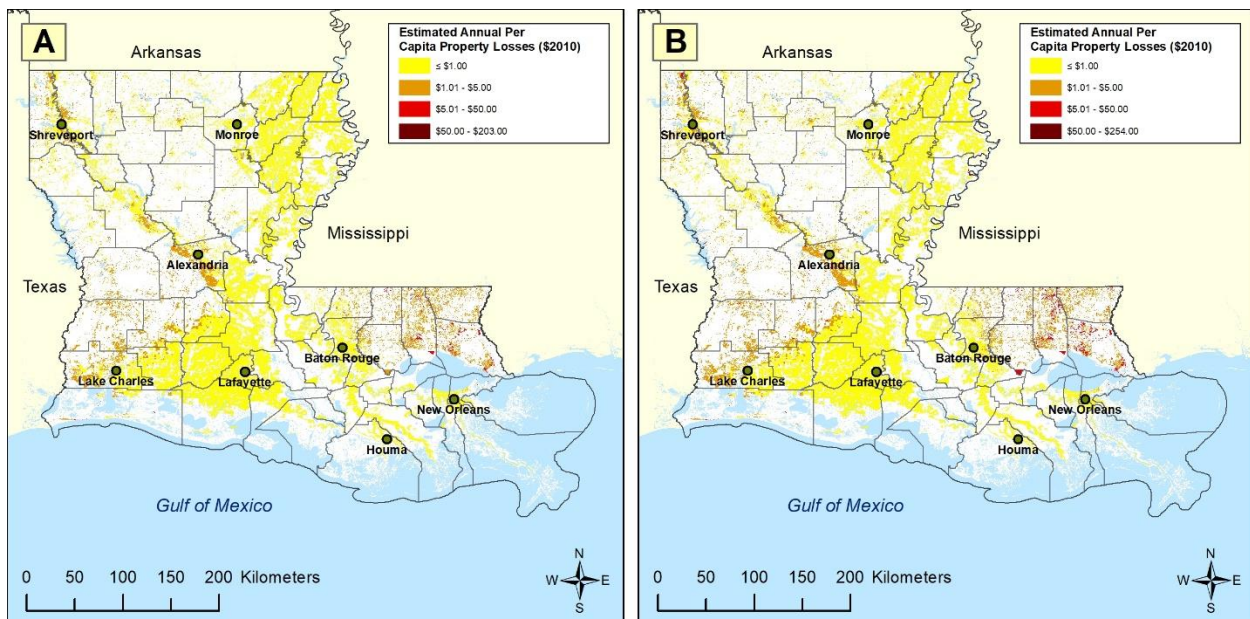


Figure 4| Estimated annual per capita property loss (\$2010) due to wildfire by census block: (A) historical (1992–2015), and (B) 2050.

At the parish level, St. Tammany (in east-central Louisiana) had the highest historical (1992–2015) overall wildfire annual property loss (\$890,955), per capita property loss (\$3.81), and per building property loss (\$9.34) among the parishes (Appendix D). Changes in the wildfire burn probability and expansion of population are projected to change wildfire risk by 2050. Nevertheless, the greatest annual wildfire property loss (\$2,646,673), per capita property loss (\$4.76), and per building property loss (\$11.68) are expected to remain in St. Tammany Parish (Appendix D).

At the census-block level, the highest historical average annual property loss due to wildfire was in block 221030408035041 of St. Tammany Parish (\$10,764). The highest historical (1992–2015) average annual per building property loss (\$21.34) was in census block 221030407061032, also in St. Tammany Parish. The highest historical annual per capita property loss in the state was \$202.76 in census block 220919511002011, in St. Helena Parish (east-central Louisiana, northwest of St. Tammany).

By 2050, the highest annual property loss due to wildfire is projected to be in census block 221030408035041, in St. Tammany Parish (\$31,972). The highest annual per capita property loss (\$253.45) will be in census block 220919511002011 of St. Helena Parish. The highest annual per building property loss (\$26.68) will be in census block 221030407061032, in St. Tammany Parish.

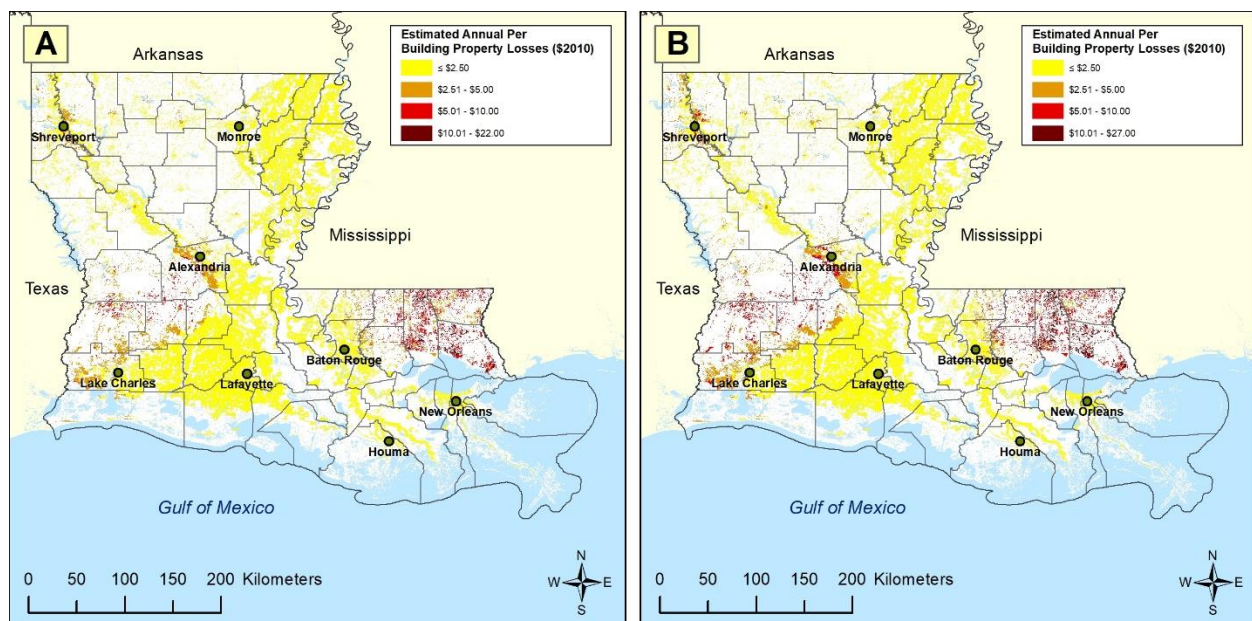


Figure 5 | Estimated annual per building property loss: (A) historical (1992–2015), and (B) 2050 by census block in Louisiana (\$2010).

DISCUSSION

While it is tempting to overlook the wildfire hazard in a state that receives abundant rainfall, is susceptible to so many other, more calamitous hazards, and often suffers from other more pressing economic hardships, the wildfire hazard in Louisiana is formidable, and is expected to become more destructive in coming decades. Thus, adequate resources should be devoted to

preventing and mitigating the hazard, including but not limited to, educating the public on the dangers of carelessness with managed fires. Additional resources will be needed to combat the anticipated increased risk. The fact that no major spatial shifts in the wildfire hazard were found simplifies planning for the wildfire hazard over the coming decades. The hope is that any reductions in ability to acquire resources to prevent or mitigate the hazard are offset by improvements and innovations in technology to detect and combat the fires. If the risk does indeed remain roughly proportionate to the population increase, resources to combat the risk should be available, assuming that other economic and demographic factors also change proportionately. For example, the vulnerability to wildfire under the uncertain and complex conditions of response during the COVID-19 pandemic would almost certainly exacerbate losses (Thompson et al. 2021).

LIMITATION

As in any research, this work has some caveats that should be acknowledged. One set of limitations involves the population projection methodology, which ignores abrupt changes in the future, such as migrations prompted by hurricanes or other natural disasters, economic depression, or other extreme events. Another limitation is the assumption, necessitated by data availability, of equal population growth rates for every census block within a parish. In addition, population growth may not follow an exponential growth curve. This research also does not consider changes in economic and demographic characteristics by 2050, which might alter the ability for taxes to cover additional mitigation and prevention strategies. Unfortunately, the absence of reliable demographic projections for Louisiana based on more elaborate modeling makes these assumptions necessary.

The lack of consideration of other non-population-related features can also limit the reliability of the findings. This work does not consider land cover change, which might change the future potential destructiveness of the fires. Furthermore, in calculating the losses, building replacement/renovation/restoration cost rather than building value could have given additional information that would have assisted in some aspects of planning, such as for setting fire insurance premiums.

SUMMARY AND CONCLUSION

This research has developed a method for analyzing historical and future property losses to wildfire in Louisiana, a U.S. state with relatively dense population, rich timber resources, and a likely increasing susceptibility to long periods without rainfall. In contrast to most work on spatial distribution of hazards, the analysis is done at the census-block level, which provides a more suitable areal unit of analysis than the parish (i.e., county) because of the wide disparities in population, property, and (in some cases) natural vulnerability to the hazard. The results suggest that the present areas of maximum risk – west-central, east-central, and extreme northwestern and southwestern coastal Louisiana – will remain the most vulnerable areas to this often-overlooked hazard in 2050. However, annual loss, both on an absolute and per capita basis, are expected to increase substantially, as the population growth, WUI and climate change combine to exacerbate the risk.

Future research should be conducted to extend a similar methodology to other hazards in other places, such as earthquakes, sinkholes, lightning, and hail. In a more general sense, improved population, economic, and demographic forecasts are needed, so that current and future risk to natural hazards, including wildfire, can be assessed more accurately. As climate models become more accurate, the reliability of future projections for natural hazard risk will improve in their mission of protecting lives and property.

DATA AVAILABILITY STATEMENT

The raw data supporting the conclusions of this article will be made available by the authors, without undue reservation.

AUTHORS' CONTRIBUTIONS

RM developed the methodology, collected and analyzed the data, and developed the initial text. CF provided original ideas and advice on the overall project methodology and edited the text. RR developed the atmospheric projections and edited early and late drafts of the text. NB expanded the literature review and provided oversight on analysis, particularly regarding the population projections.

FUNDING

This project resulted from the 2019 Louisiana State Hazard Mitigation Plan update, for which CF and RR received funding from FEMA, via Louisiana's Governor's Office of Homeland Security and Emergency Preparedness (GOHSEP), grant number: 2000301135. Any opinions, findings, conclusions, and recommendations expressed in this manuscript are those of the authors and do not necessarily reflect the views of FEMA or GOHSEP.

ACKNOWLEDGMENT

Publication of this article was subsidized by the LSU Libraries Open Access Author Fund. The authors warmly appreciate the assistance and support of Jeffrey Giering of GOHSEP for overall project support, and David Dunaway of LSU Libraries for assistance in acquiring population data. Bret Lane of Louisiana Department of Agriculture and Forestry provided wildfire damage data.

REFERENCES

- Abatzoglou, J. T., and Williams, A. P. (2016). Impact of anthropogenic climate change on wildfire across western US forests. *Proceedings of the National Academy of Sciences*, 113(42), 11770–11775, doi: 10.1073/pnas.1607171113
- Ager, A. A., Buonopane, M., Reger, A., and Finney, M. A. (2013). Wildfire exposure analysis on the national forests in the Pacific Northwest, USA. *Risk Analysis*, 33(6), 1000–1020, doi: 10.1111/j.1539-6924.2012.01911.x
- Ager, A. A., Day, M. A., Alcasena, F. J., Evers, C. R., Short, K. C., and Grenfell, I. (2021). Predicting paradise: Modeling future wildfire disasters in the western US. *Science of the Total Environment*, 784, Art. No. 147057, doi: 10.1016/j.scitotenv.2021.147057
- Ager, A. A., Kline, J. D., and Fischer, A. P. (2015). Coupling the biophysical and social dimensions of wildfire risk to improve wildfire mitigation planning. *Risk Analysis*, 35(8), 1393–1406, doi: 10.1111/risa.12373
- Ager, A. A., Preisler, H. K., Arca, B., Spano, D., and Salis, M. (2014). Wildfire risk estimation in the Mediterranean area. *Environmetrics*, 25(6), 384–396, doi: 10.1002/env.2269
- Alcasena, F. J., Salis, M., and Vega-García, C. (2016). A fire modeling approach to assess wildfire exposure of valued resources in central Navarra, Spain. *European Journal of Forest Research*, 135(1), 87–107, doi: 10.1007/s10342-015-0919-6
- Aldersley, A., Murray, S. J., and Cornell, S. E. (2011). Global and regional analysis of climate and human drivers of wildfire. *Science of the Total Environment*, 409(18), 3472–3481, doi: 10.1016/j.scitotenv.2011.05.032
- Ayres, A., Degolia, A., Fienup, M., Kim, Y., Sainz, J., Urbisci, L., Viana, D., Wesolowski, G., Plantinga, A.J., and Tague, C. (2016). Social science/natural science perspectives on wildfire and climate change. *Geography Compass*, 10(2), 67–86, doi: 10.1111/gec3.12259
- Binkley, D., Sisk, T., Chambers, C., Springer, J., and Block, W. (2007). The role of old-growth forests in frequent-fire landscapes. *Ecology and Society*, 12(2), 18. [online] URL: <http://www.ecologyandsociety.org/vol12/iss2/art18/>
- Bui, D. T., Bui, Q. T., Nguyen, Q. P., Pradhan, B., Nampak, H., and Trinh, P. T. (2017). A hybrid artificial intelligence approach using GIS-based neural-fuzzy inference system and particle swarm optimization for forest fire susceptibility modeling at a tropical area. *Agricultural and Forest Meteorology*, 233, 32–44, doi: 10.1016/j.agrformet.2016.11.002
- Bushra, N., Rohli, R. V., Lam, N. S., Zou, L., Mostafiz, R. B., and Mihunov, V. (2019). The relationship between the normalized difference vegetation index and drought indices in the South Central United States. *Natural Hazards*, 96(2), 791–808, doi: 10.1007/s11069-019-03569-5

- Butry, D. T., Mercer, E. D., Prestemon, J. P., Pye, J. M., and Holmes, T. P. (2001). What is the price of catastrophic wildfire? *Journal of Forestry*, 99(11), 9–17. Available at: https://www.srs.fs.usda.gov/pubs/ja/ja_butry001.pdf. Last accessed: 07/08/2021
- Cannon, S. H., and DeGraff, J. (2009). The increasing wildfire and post-fire debris-flow threat in western USA, and implications for consequences of climate change. In: Sassa K., Canuti P. (eds) *Landslides–Disaster Risk Reduction* (pp. 177–190). Springer, Berlin, Heidelberg, doi: 10.1007/978-3-540-69970-5_9
- Catry, F. X., Rego, F. C., Bação, F. L., and Moreira, F. (2010). Modeling and mapping wildfire ignition risk in Portugal. *International Journal of Wildland Fire*, 18(8), 921–931, doi: 10.1071/WF07123
- Cleland, D. T., Crow, T. R., Saunders, S. C., Dickmann, D. I., Maclean, A. L., Jordan, J. K., Watson, R. L., Sloan, A. M., Brososke, and K. D (2004). Characterizing historical and modern fire regimes in Michigan (USA): a landscape ecosystem approach. *Landscape Ecology*, 19(3), 311–325. Available at: https://www.srs.fs.usda.gov/pubs/ja/ja_cleland001.pdf. Last accessed: 07/08/2021
- Colantoni, A., Egidi, G., Quaranta, G., D’Alessandro, R., Vinci, S., Turco, R., and Salvati, L. (2020). Sustainable Land Management, Wildfire Risk and the Role of Grazing in Mediterranean Urban-Rural Interfaces: A Regional Approach from Greece. *Land*, 9(1), 21, doi: 10.3390/land9010021
- Coleman, T. W., Meeker, J. R., Clarke, S. R., and Rieske, L. K. (2008). The suppression of *Dendroctonus frontalis* and subsequent wildfire have an impact on forest stand dynamics. *Applied Vegetation Science*, 11(2), 231–242, doi: 10.3170/2008-7-18362
- Davis, K. T., Dobrowski, S. Z., Higuera, P. E., Holden, Z. A., Veblen, T. T., Rother, M. T., Parks, S.A., Sala, A., and Maneta, M. P. (2019). Wildfires and climate change push low-elevation forests across a critical climate threshold for tree regeneration. *Proceedings of the National Academy of Sciences*, 116(13), 6193–6198, doi: 10.1073/pnas.1815107116
- De la Riva, J., Pérez-Cabello, F., Lana-Renault, N., and Koutsias, N. (2004). Mapping wildfire occurrence at regional scale. *Remote Sensing of Environment*, 92(3), 363–369, doi: 10.1016/j.rse.2004.06.022
- de Zea Bermudez, P., Mendes, J., Pereira, J. M. C., Turkman, K. F., and Vasconcelos, M. J. P. (2010). Spatial and temporal extremes of wildfire sizes in Portugal (1984–2004). *International Journal of Wildland Fire*, 18(8), 983–991, doi: 10.1071/WF07044
- Dennison, P. E., Brewer, S. C., Arnold, J. D., and Moritz, M. A. (2014). Large wildfire trends in the western United States, 1984–2011. *Geophysical Research Letters*, 41(8), 2928–2933, doi: 10.1002/2014GL059576

- Dillon, G., Menakis, J., and Fay, F. (2015). Wildland fire potential: a tool for assessing wildfire risk and fuels management needs. In: *Keane, Robert E.; Jolly, Matt; Parsons, Russell; Riley, Karin. Proceedings of the large wildland fires conference; May 19-23, 2014; Missoula, MT. Proc. RMRS-P-73. Fort Collins, CO: US Department of Agriculture, Forest Service, Rocky Mountain Research Station. p. 60-76. (Vol. 73, pp. 60–76). Available at: https://www.fs.fed.us/rm/pubs/rmrs_p073/rmrs_p073_060_076.pdf. Last accessed: 07/08/2021*
- Drewa, P. B., Platt, W. J., and Moser, E. B. (2002). Fire effects on resprouting of shrubs in headwaters of southeastern longleaf pine savannas. *Ecology*, 83(3), 755–767, doi: 10.1890/0012-9658(2002)083[0755:FEOROS]2.0.CO;2
- Enright, N. J., and Fontaine, J. B. (2014). Climate Change and the Management of Fire-Prone Vegetation in Southwest and Southeast Australia. *Geographical Research*, 52(1), 34–44, doi: 10.1111/1745-5871.12026
- Ergibi, M., and Hessel, H. (2020). Awareness and adoption of FireSmart Canada: Barriers and incentives. *Forest Policy and Economics*, 119, Art. No. 102271, doi: 10.1016/j.forpol.2020.102271
- Fann, N., Alman, B., Broome, R. A., Morgan, G. G., Johnston, F. H., Pouliot, G., and Rappold, A. G. (2018). The health impacts and economic value of wildland fire episodes in the US: 2008–2012. *Science of the Total Environment*, 610, 802–809, doi: 10.1016/j.scitotenv.2017.08.024
- Finney, M. A., McHugh, C. W., Grenfell, I. C., Riley, K. L., and Short, K. C. (2011). A simulation of probabilistic wildfire risk components for the continental United States. *Stochastic Environmental Research and Risk Assessment*, 25(7), 973–1000, doi: 10.1007/s00477-011-0462-z
- Flannigan, M. D., Krawchuk, M. A., de Groot W. J., Wotton B. M., and Gowman L. M. (2009). Implications of changing climate for global wildland fire. *International Journal of Wildland Fire*, 18, 483–507 doi: 10.1071/WF15083
- Frankson, R., Kunkel, K., and Champion, S. (2017). Louisiana State Climate Summary. NOAA Technical Report NESDIS 149-LA, March 2019 Revision, 4 pp. Available at: <https://statesummaries.ncics.org/chapter/la/>. Last accessed: 07/08/2021
- Gannon, C. S., and Steinberg, N. C. (2021). A global assessment of wildfire potential under climate change utilizing Keetch-Byram drought index and land cover classifications. *Environmental Research Communications*, 3(3), Art. No. 035002, doi: 10.1088/2515-7620/abd836
- Grala, K., and Cooke, W. H. (2010). Spatial and temporal characteristics of wildfires in Mississippi, USA. *International Journal of Wildland Fire*, 19(1), 14–28, doi: 10.1071/WF08104
- Hamilton, M., and Salerno, J. (2020). Cognitive maps reveal diverse perceptions of how prescribed fire affects forests and communities. *Frontiers in Forests and Global Change*, 3, Art. No. 75, doi: 10.3389/ffgc.2020.00075

- Hansen, W. D., Mueller, J. M., and Naughton, H. T. (2014). Wildfire in hedonic property value studies. *Western Economics Forum, Western Agricultural Economics Association*, 13(1), 23–35, doi: 10.22004/ag.econ.189736
- Haywood, J. D. (2011). Influence of herbicides and felling, fertilization, and prescribed fire on longleaf pine growth and understory vegetation through ten growing seasons and the outcome of an ensuing wildfire. *New Forests*, 41(1), 55–73, doi: 10.1007/s11056-010-9209-9
- Haywood, J. D., Pearson, H. A., Grelen, H. E., and Popham, T. W. (2000). Effects of date and frequency of burning on southern bayberry (*Myrica cerifera*) in central Louisiana. *Texas Journal of Science*. 52 (4) Supplement: 33–42. Available at: https://www.srs.fs.usda.gov/pubs/ja/ja_haywood008.pdf. Last accessed: 07/08/2021
- Higuera, P. E., Abatzoglou, J. T., Littell, J. S., and Morgan, P. (2015). The changing strength and nature of fire-climate relationships in the northern Rocky Mountains, U.S.A., 1902–2008. *PLoS ONE*, 10, e0127563, doi: 10.1371/journal.pone.0127563.
- Holden, Z. A., Swanson, A., Luce, C. H., Jolly, W. M., Maneta, M., Oyler, J. W., Warren, D. A., Parsons, R., and Affleck, D. (2018). Decreasing fire season precipitation increased recent western US forest wildfire activity. *Proceedings of the National Academy of Sciences*, 115(36), E8349–E8357, doi: 10.1073/pnas.1802316115
- Hood, S. M., Keyes, C. R., Bowen, K. J., Lutes, D. C., and Seielstad, C. (2020). Fuel treatment longevity in ponderosa pine-dominated forest 24 years after cutting and prescribed burning. *Frontiers in Forests and Global Change*, 3, 78, doi: 10.3389/ffgc.2020.00078
- Hong, H., Jaafari, A., and Zenner, E. K. (2019). Predicting spatial patterns of wildfire susceptibility in the Huichang County, China: An integrated model to analysis of landscape indicators. *Ecological Indicators*, 101, 878–891, doi: 10.1016/j.ecolind.2019.01.056
- Jaafari, A., Zenner, E. K., and Pham, B. T. (2018). Wildfire spatial pattern analysis in the Zagros Mountains, Iran: A comparative study of decision tree based classifiers. *Ecological informatics*, 43, 200–211, doi: 10.1016/j.ecoinf.2017.12.006
- Jaafari, A., Termeh, S. V. R., and Bui, D. T. (2019a). Genetic and firefly metaheuristic algorithms for an optimized neuro-fuzzy prediction modeling of wildfire probability. *Journal of Environmental Management*, 243, 358–369, doi: 10.1016/j.jenvman.2019.04.117
- Jaafari, A., Zenner, E. K., Panahi, M., and Shahabi, H. (2019b). Hybrid artificial intelligence models based on a neuro-fuzzy system and metaheuristic optimization algorithms for spatial prediction of wildfire probability. *Agricultural and Forest Meteorology*, 266, 198–207, doi: 10.1016/j.agrformet.2018.12.015
- Jones, J. D., and Chamberlain, M. J. (2004). Efficacy of herbicides and fire to improve vegetative conditions for northern bobwhites in mature pine forests. *Wildlife Society Bulletin*, 32(4), 1077–1084, doi: 10.2193/0091-7648(2004)032[1077:EOHAFT]2.0.CO;2

- Jones, S. F., Stagg, C. L., Yando, E. S., James, W. R., Buffington, K. J., and Hester, M. W. (2020). Stress gradients interact with disturbance to reveal alternative states in salt marsh: Multivariate resilience at the landscape scale. *Journal of Ecology*, doi: 10.1111/1365-2745.13552
- Kaulfus, A. S., Nair, U., Jaffe, D., Christopher, S. A., and Goodrick, S. (2017). Biomass burning smoke climatology of the United States: Implications for particulate matter air quality. *Environmental Science & Technology*, 51(20), 11731–11741, doi: 10.1021/acs.est.7b03292
- Krueger, E.S., Ochsner, T.E., Quiring, S.M., Engle, D.M., Carlson, J.D., Twidwell, D., and Fuhlendorf, S.D. (2017). Measured soil moisture is a better predictor of large growing-season wildfires than the Keetch-Byram Drought Index. *Soil Science Society of America Journal*, 81, 490–502. doi: 10.2136/sssaj2017.01.0003.
- Lasslop, G., and Kloster, S. (2017). Human impact on wildfires varies between regions and with vegetation productivity. *Environmental Research Letters*, 12(11), 115011, doi: 10.1088/1748-9326/aa8c82
- Li, L. M., Song, W. G., Ma, J., and Satoh, K. (2009). Artificial neural network approach for modeling the impact of population density and weather parameters on forest fire risk. *International Journal of Wildland Fire*, 18(6), 640–647, doi: 10.1071/WF07136
- Liu, Y., Stanturf, J.A., and Goodrick, S.L. (2009). Trends in global wildfire potential in a changing climate. *Forest Ecology and Management*, 259(4), 685–697, doi: 10.1016/j.foreco.2009.09.002
- Louisiana Department of Agriculture & Forestry. (2021). Forestry Protection. Available at <https://www.ldaf.state.la.us/forestry/protection/>. Last accessed: 6/25/2021.
- Magnée, J. (2020). The Effect of Wildfire Risk on Residential Property Values in the Netherlands. M.S. Thesis. Maastricht University, Available at: <https://finance-ideas.nl/wp-content/uploads/2020/09/the-effect-of-wildfire-risk-on-residential-property-values-in-the-netherlands.pdf>. Last accessed: 6/19/2021.
- Malamud, B. D., Millington, J. D., and Perry, G. L. (2005). Characterizing wildfire regimes in the United States. *Proceedings of the National Academy of Sciences*, 102(13), 4694–4699, doi: 10.1073/pnas.0500880102
- Marlon, J. R., Bartlein, P. J., Walsh, M. K., Harrison, S. P., Brown, K. J., Edwards, M. E., Higuera, P. E., Power, M. J., Anderson, R. S., Briles, C., Brunelle, A., Carcaillet, C., Daniels, M., Hu, F. S., Lavoie, M., Long, C., Minckley, T., Richard, P. J. H., Scott, A. C., Shafer, D. S., Tinner, W., Umbanhowar Jr, C. E., and Whitlock, C. (2009). Wildfire responses to abrupt climate change in North America. *Proceedings of the National Academy of Sciences*, 106(8), 2519–2524, doi: 10.1073/pnas.0808212106
- McCoy, S. J., and Walsh, R. P. (2018). Wildfire risk, salience & housing demand. *Journal of Environmental Economics and Management*, 91(2018), 203–228, doi: 10.1016/j.jeem.2018.07.005

- Mokhov, I. I., Chernokulsky, A. V., and Shkolnik, I. M. (2006). Regional model assessments of fire risks under global climate changes. *Doklady Earth Sciences*, 411A(9), 1485–1488, doi: 10.1134/S1028334X06090340
- Moreira, F., Vaz, P., Catry, F., and Silva, J. S. (2009). Regional variations in wildfire susceptibility of land-cover types in Portugal: implications for landscape management to minimize fire hazard. *International Journal of Wildland Fire*, 18(5), 563–574 doi: 10.1071/WF07098
- Morgan, P., Hardy, C. C., Swetnam, T. W., Rollins, M. G., and Long, D. G. (2001). Mapping fire regimes across time and space: understanding coarse and fine-scale fire patterns. *International Journal of Wildland Fire*, 10(4), 329–342 doi: 10.1071/WF01032
- Moritz, M. A. (2012). Wildfires ignite debate on global warming. *Nature News*, 487(7407), 273, doi: 10.1038/487273a
- Mostafiz, R. B., Friedland, C. J., Rohli, R. V., Gall, M., Bushra, N., and Gilliland, J. M. (2020). Census-Block-Level Property Risk Estimation Due to Extreme Cold Temperature, Hail, Lightning, and Tornadoes in Louisiana, United States. *Frontiers in Earth Science*, 8, Art. No. 601624, doi: 10.3389/feart.2020.601624
- O’Gorman, P. A., and Schneider, T. (2009). The physical basis for increases in precipitation extremes in simulations of 21st-century climate change. *Proceedings of the National Academy of Sciences of the United States of America*, 106(35), 14773–14777, doi: 10.1073/pnas.0907610106
- Papakosta, P., Xanthopoulos, G., and Straub, D. (2017). Probabilistic prediction of wildfire economic losses to housing in Cyprus using Bayesian network analysis. *International Journal of Wildland Fire*, 26(1), 10–23, doi: 10.1071/WF15113
- Penman, T. D., Clarke, H., Cirulis, B., Boer, M. M., Price, O. F., and Bradstock, R. A. (2020). Cost-effective prescribed burning solutions vary between landscapes in eastern Australia. *Frontiers in Forests and Global Change*, 3, Art. No. 79, doi: 10.3389/ffgc.2020.00079
- Pharo, J. A., and Croom, E. L. (1971). Correlation between Keetch-Byram drought index and wildfire statistics. *Bulletin of the American Meteorological Society*, 52(3), 205.
- Piñol, J., Terradas, J., and Lloret, F. (1998). Climate warming, wildfire hazard, and wildfire occurrence in coastal eastern Spain. *Climatic Change*, 38, 345–357, doi: 10.1023/A:1005316632105
- Pope, V., Gallani, M.L., Rowntree, P.R., and Stratton, R.A. (2000). The impact of new physical parameterizations in the Hadley Centre climate model: HadAM3. *Climate Dynamics*, 16(2–3), 123–146, doi: 10.1007/s003820050009
- Preisler, H. K., Brillinger, D. R., Burgan, R. E., and Benoit, J. W. (2004). Probability based models for estimation of wildfire risk. *International Journal of Wildland Fire*, 13(2), 133–142, doi: 10.1071/WF02061
- Prestemon, J.P., Shankar, U., Xiu, A., Talgo, K., Yang, D., Dixon, E., McKenzie, D., and Abt, K.L. (2016). Projecting wildfire area burned in the south-eastern United States, 2011–60. *International Journal of Wildland Fire*, 25(7), 715–729, doi: 10.1071/WF15124

- Radeloff, V. C., Hammer, R. B., Stewart, S. I., Fried, J. S., Holcomb, S. S., and McKeefry, J. F. (2005). The wildland-urban interface in the United States. *Ecological Applications*, 15(3), 799–805, doi: 10.1890/04-1413
- Running, S. W. (2006). Is global warming causing more, larger wildfires? *Science*, 313(5789), 927–928, doi: 10.1126/science.1130370.
- Schoennagel, T., Veblen, T. T., and Romme, W. H. (2004). The interaction of fire, fuels, and climate across Rocky Mountain forests. *BioScience*, 54(7), 661–676, doi: 10.1641/0006-3568(2004)054[0661:TIOFFA]2.0.CO;2
- Schubert, S. D., Chang, Y., DeAngelis, A. M., Wang, H., and Koster, R. D. (2021). On the development and demise of the Fall 2019 Southeast US flash drought: Links to an extreme positive IOD. *Journal of Climate*, 34(5), 1701–1723, doi: 10.1175/JCLI-D-20-0428.1
- Short, K. C., Finney, M. A., Scott, J. H., Gilbertson-Day, J. W., and Grenfell, I. C. (2016). Spatial dataset of probabilistic wildfire risk components for the conterminous United States. 1st Edition. Fort Collins, CO: Forest Service Research Data Archive, doi: 10.2737/RDS-2016-0034
- Short, K. C. (2017). Spatial wildfire occurrence data for the United States, 1992–2015 [FPA_FOD_20170508]. 4th Edition. Fort Collins, CO: Forest Service Research Data Archive, doi: 10.2737/RDS-2013-0009.4
- Short, K. C., Finney, M. A., Vogler, K. C., Scott, J. H., Gilbertson-Day, J. W., and Grenfell, I. C. (2020). Spatial datasets of probabilistic wildfire risk components for the United States (270m). 2nd Edition. Fort Collins, CO: Forest Service Research Data Archive, doi: 10.2737/RDS-2016-0034-2
- Short, K. C. (2013). Spatial wildfire occurrence data for the United States, 1992–2011 [FPA_FOD_20130422]. 1st Edition. Fort Collins, CO: U.S. Department of Agriculture, Forest Service, Rocky Mountain Research Station, doi: 10.2737/RDS-2013-0009
- Silverman, B. W. (1986). *Density Estimation for Statistics and Data Analysis*. New York: Chapman and Hall.
- Simmons, S. A., and Bossart, J. L. (2020). Apparent resilience to fire of native bee (Hymenoptera: Apoidea) communities from upland longleaf pine forests in Louisiana and Mississippi. *Southeastern Naturalist*, 19(3), 567–581, doi: 10.1656/058.019.0316
- Sorensen, C., House, J. A., O'Dell, K., Brey, S. J., Ford, B., Pierce, J. R., Fischer, E. V., Lemery, J., and Crooks, J. L. (2021). Associations between wildfire-related PM2.5 and intensive care unit admissions in the United States, 2006–2015. *GeoHealth*, 5(5), Art, No. e2021GH000385, doi: 10.1029/2021GH000385
- Stambaugh, M. C., Guyette, R. P., and Marschall, J. M. (2011). Longleaf pine (*Pinus palustris* Mill.) fire scars reveal new details of a frequent fire regime. *Journal of Vegetation Science*, 22(6), 1094–1104, doi: 10.1111/j.1654-1103.2011.01322.x

- Strydom, S., and Savage, M. J. (2017). Potential impacts of climate change on wildfire dynamics in the midlands of KwaZulu-Natal, South Africa. *Climatic Change*, 143(3), 385–397, doi: 10.1007/s10584-017-2019-8
- Theobald, D. M., and Romme, W. H. (2007). Expansion of the US wildland–urban interface. *Landscape and Urban Planning*, 83(4), 340–354, doi: 10.1016/j.landurbplan.2007.06.002
- Thompson, M. P., Scott, J., Kaiden, J. D., and Gilbertson-Day, J. W. (2013). A polygon-based modeling approach to assess exposure of resources and assets to wildfire. *Natural Hazards*, 67(2), 627–644, doi: 10.1007/s11069-013-0593-2
- Thompson, M. P., Belval, E. J., Dilliot, J., and Bayham, J. (2021). Supporting wildfire response during a pandemic in the United States: The COVID-19 incident risk assessment tool. *Frontiers in Forests and Global Change*, 4, doi: 10.3389/ffgc.2021.655493
- Tutmez, B., Ozdogan, M. G., and Boran, A. (2018). Mapping forest fires by nonparametric clustering analysis. *Journal of Forestry Research*, 29(1), 177–185, doi: 10.1007/s11676-017-0417-4
- United States Census of Agriculture. (2017). Short rotation woody crops: 2017 and 2012. Table 36, p. 617. Available at: https://www.nass.usda.gov/Publications/AgCensus/2017/Full_Report/Volume_1,_Chapter_2_US_State_Level/usv1.pdf
- United States Census Bureau. (2021). Available at: <https://www2.census.gov/programs-surveys/popest/datasets/> Last accessed: 6/20/2021.
- United States Census Bureau. (2010). TIGER/Line Shapefiles. Available at: <https://www.census.gov/geographies/mapping-files/time-series/geo/tiger-line-file.2010.html> Last accessed: 06/21/2021.
- United States Global Change Research Program. (2017). Climate science special report: Fourth national climate assessment, Volume I. Editors Wuebbles, D. J., Fahey, D. W., Hibbard, K. A., Dokken, D. J., Stewart, B. C., and Maycock, T. K. (Washington, D.C., United States: U.S. Global Change Research Program), 470 pp., doi: 10.7930/J0J964J6
- Vautard, R., and Yiou, P. (2009). Control of recent European surface climate change by atmospheric flow. *Geophysical Research Letters*, 36(22), Art. No. L22702, doi: 10.1029/2009GL040480
- Vázquez, A., Pérez, B., Fernández-González, F., and Moreno, J. M. (2002). Recent fire regime characteristics and potential natural vegetation relationships in Spain. *Journal of Vegetation Science*, 13(5), 663–676, doi: 10.1111/j.1654-1103.2002.tb02094.x
- WebWIMP Water Balance Calculator. (2021). Available at: <http://climate.geog.udel.edu/~climate/>. Last accessed: 6/30/2021.
- Wehner, M. F., Arnold, J. R., Knutson, T., Kunkel, K. E., and LeGrande, A. N. (2017). Droughts, floods, and wildfires. In: Climate Science Special Report: Fourth National Climate Assessment, Volume I [Wuebbles, D. J., Fahey, D. W., Hibbard, K. A., Dokken, D. J., Stewart, B. C., and Maycock, T. K. (eds.)]. U.S. Global Change Research Program, Washington, DC, USA, pp. 231–256. doi: 10.7930/J0CJ8BNN.

- Westerling, A. L. (2016). Increasing western US forest wildfire activity: Sensitivity to changes in the timing of spring. *Philosophical Transactions of the Royal Society B: Biological Sciences*, 371(1696), Art. No. 20150178, doi: 10.1098/rstb.2015.0178
- Westerling, A. L., Hidalgo, H. G., Cayan, D. R. and Swetnam, T. W. (2006). Warming and earlier spring increase western U.S. forest wildfire activity. *Science*, 313(5789), 940–943, doi: 10.1126/science.1128834
- Willmott, C.J., Rowe, C. M., and Mintz, Y. (1985). Climatology of the terrestrial seasonal water cycle. *Journal of Climatology*, 5(6), 589–606, doi: 10.1002/joc.3370050602
- Yeldell, N. A., Cohen, B. S., Prebyl, T. J., Collier, B. A., and Chamberlain, M. J. (2017). Prescribed fire influences habitat selection of female eastern wild turkeys. *Journal of Wildlife Management*, 81(7), 1287–1297, doi: 10.1002/jwmg.21290

SUPPLEMENTARY MATERIALS

Appendix A: Historical (1992–2015) Wildfire Burn Probability (%) in 2050, by Louisiana Parish.

Parish	Point-based		Parishwide	
	Min	Max	Mean	Standard Deviation
Acadia	0.01	1.18	0.16	0.18
Allen	1.20	6.22	3.77	1.28
Ascension	0.01	1.04	0.36	0.24
Assumption	0.00	0.05	0.01	0.01
Avoyelles	0.06	1.23	0.29	0.21
Beauregard	2.01	5.39	3.87	0.47
Bienville	0.82	1.52	1.17	0.14
Bossier	0.71	2.06	1.14	0.24
Caddo	0.65	3.20	1.59	0.56
Calcasieu	0.13	6.48	1.82	1.07
Caldwell	0.45	1.64	0.99	0.27
Cameron	0.00	7.70	1.52	1.61
Catahoula	0.07	1.24	0.53	0.31
Claiborne	1.11	1.56	1.37	0.11
Concordia	0.06	0.46	0.18	0.08
De Soto	0.61	1.72	0.83	0.20
East Baton Rouge	0.05	2.92	0.64	0.54
East Carroll	0.06	0.36	0.21	0.07
East Feliciana	0.15	3.67	1.72	0.86
Evangeline	0.25	5.23	1.73	1.06
Franklin	0.07	0.78	0.24	0.14
Grant	1.18	2.07	1.74	0.20
Iberia	0.00	0.02	0.00	0.00
Iberville	0.00	0.36	0.03	0.04
Jackson	0.84	1.22	1.03	0.08
Jefferson	0.00	0.93	0.13	0.18
Jefferson Davis	0.04	2.52	0.72	0.56
Lafayette	0.01	0.09	0.02	0.01
Lafourche	0.00	0.08	0.01	0.01
LaSalle	0.32	2.01	1.45	0.37
Lincoln	0.85	1.33	1.07	0.12
Livingston	0.51	4.41	2.15	0.95
Madison	0.06	0.33	0.13	0.06
Morehouse	0.30	0.96	0.64	0.14

Natchitoches	0.82	1.74	1.13	0.15
Orleans	0.08	2.31	0.93	0.54
Ouachita	0.37	0.89	0.64	0.13
Plaquemines	0.00	0.24	0.03	0.05
Pointe Coupee	0.03	0.17	0.08	0.03
Rapides	0.47	6.13	2.43	1.46
Red River	0.65	1.03	0.83	0.08
Richland	0.22	0.67	0.34	0.07
Sabine	0.81	2.16	1.35	0.30
St. Bernard	0.00	2.00	0.24	0.21
St. Charles	0.00	0.49	0.05	0.06
St. Helena	2.17	4.75	3.97	0.48
St. James	0.01	0.50	0.10	0.10
St. John the Baptist	0.01	1.47	0.46	0.37
St. Landry	0.03	0.76	0.17	0.13
St. Martin	0.00	0.06	0.01	0.01
St. Mary	0.00	0.01	0.00	0.00
St. Tammany	0.92	5.60	3.15	0.89
Tangipahoa	1.22	4.76	3.55	0.96
Tensas	0.06	0.68	0.18	0.12
Terrebonne	0.00	0.02	0.00	0.00
Union	0.65	1.22	0.89	0.12
Vermilion	0.00	0.53	0.04	0.06
Vernon	1.34	6.11	3.08	1.12
Washington	3.19	6.93	4.14	0.69
Webster	0.97	1.54	1.34	0.10
West Baton Rouge	0.02	0.19	0.07	0.04
West Carroll	0.19	0.56	0.39	0.07
West Feliciana	0.06	1.39	0.34	0.26
Winn	1.10	1.98	1.48	0.21

Appendix B: Projected Wildfire Burn Probability (%) in 2050, by Louisiana Parish.

NAME	Point-based		Parishwide	
	Min	Max	Mean	Standard Deviation
Acadia	0.01	1.47	0.20	0.22
Allen	1.50	7.77	4.71	1.60
Ascension	0.02	1.30	0.45	0.30
Assumption	0.00	0.06	0.01	0.01
Avoyelles	0.08	1.54	0.36	0.26
Beauregard	2.51	6.73	4.83	0.59
Bienville	1.03	1.89	1.47	0.17
Bossier	0.89	2.57	1.43	0.31
Caddo	0.81	4.00	1.99	0.70
Calcasieu	0.16	8.10	2.28	1.33
Caldwell	0.56	2.05	1.23	0.33
Cameron	0.00	9.62	1.90	2.01
Catahoula	0.09	1.55	0.67	0.38
Claiborne	1.39	1.95	1.71	0.14
Concordia	0.08	0.58	0.22	0.10
De Soto	0.77	2.15	1.03	0.24
East Baton Rouge	0.06	3.65	0.80	0.67
East Carroll	0.07	0.45	0.26	0.09
East Feliciana	0.18	4.58	2.15	1.08
Evangeline	0.31	6.54	2.16	1.32
Franklin	0.08	0.98	0.29	0.17
Grant	1.47	2.59	2.17	0.25
Iberia	0.00	0.02	0.00	0.00
Iberville	0.01	0.45	0.04	0.05
Jackson	1.05	1.53	1.29	0.10
Jefferson	0.00	1.16	0.16	0.23
Jefferson Davis	0.05	3.15	0.89	0.69
Lafayette	0.01	0.11	0.03	0.02
Lafourche	0.00	0.10	0.01	0.01
LaSalle	0.40	2.51	1.81	0.47
Lincoln	1.06	1.67	1.34	0.16
Livingston	0.64	5.52	2.69	1.18
Madison	0.08	0.41	0.16	0.07
Morehouse	0.38	1.20	0.80	0.18
Natchitoches	1.02	2.18	1.42	0.18
Orleans	0.10	2.89	1.16	0.67
Ouachita	0.46	1.12	0.80	0.16

Plaquemines	0.00	0.31	0.04	0.06
Pointe Coupee	0.04	0.22	0.09	0.03
Rapides	0.59	7.66	3.04	1.83
Red River	0.81	1.29	1.04	0.10
Richland	0.27	0.83	0.43	0.09
Sabine	1.02	2.70	1.69	0.37
St. Bernard	0.00	2.50	0.30	0.26
St. Charles	0.00	0.61	0.07	0.08
St. Helena	2.71	5.94	4.96	0.60
St. James	0.01	0.62	0.13	0.12
St. John the Baptist	0.01	1.84	0.57	0.47
St. Landry	0.04	0.95	0.21	0.16
St. Martin	0.00	0.07	0.02	0.01
St. Mary	0.00	0.02	0.00	0.00
St. Tammany	1.15	7.01	3.94	1.11
Tangipahoa	1.52	5.95	4.44	1.20
Tensas	0.08	0.85	0.23	0.15
Terrebonne	0.00	0.03	0.01	0.00
Union	0.81	1.52	1.11	0.15
Vermilion	0.00	0.66	0.05	0.08
Vernon	1.68	7.64	3.85	1.40
Washington	3.99	8.67	5.18	0.87
Webster	1.21	1.93	1.67	0.13
West Baton Rouge	0.03	0.24	0.08	0.04
West Carroll	0.24	0.70	0.49	0.09
West Feliciana	0.08	1.74	0.43	0.32
Winn	1.38	2.47	1.85	0.27

Appendix C: Louisiana Parish Population in 2010, Projected Population by 2050, Density in 2010, Projected Density by 2050, and Projected Change in Population Density.

Parish	Population (2010)	Population (2050)	Density (per km ²) (2010)	Density (per km ²) (2050)	Density Change (2010–2050) (per km ²)
Acadia	61,773	67,309	36.3	39.5	3.3
Allen	25,764	30,554	13.0	15.4	2.4
Ascension	107,215	278,635	136.7	355.3	218.6
Assumption	23,421	22,875	24.8	24.2	(0.6)
Avoyelles	42,073	40,710	18.8	18.2	(0.6)
Beauregard	35,654	45,242	11.8	15.0	3.2
Bienville	14,353	11,471	6.7	5.4	(1.4)
Bossier	116,979	183,706	52.1	81.8	29.7
Caddo	254,969	238,795	105.1	98.4	(6.7)
Calcasieu	192,768	233,579	68.0	82.4	14.4
Caldwell	10,132	9,248	7.2	6.6	(0.6)
Cameron	6,839	5,253	1.4	1.0	(0.3)
Catahoula	10,407	7,741	5.4	4.0	(1.4)
Claiborne	17,195	15,467	8.7	7.8	(0.9)
Concordia	20,822	17,145	10.8	8.9	(1.9)
De Soto	26,656	28,631	11.5	12.4	0.9
East Baton Rouge	440,171	526,522	361.4	432.3	70.9
East Carroll	7,759	4,397	6.8	3.8	(2.9)
East Feliciana	20,267	20,074	17.2	17.0	(0.2)
Evangeline	33,984	33,924	19.3	19.3	(0.0)
Franklin	20,767	17,005	12.6	10.3	(2.3)
Grant	22,309	29,701	13.0	17.3	4.3
Iberia	73,240	78,687	27.4	29.5	2.0
Iberville	33,387	33,263	19.7	19.7	(0.1)
Jackson	16,274	14,727	10.8	9.8	(1.0)
Jefferson	432,552	409,450	260.1	246.2	(13.9)
Jefferson Davis	31,594	30,585	18.5	17.9	(0.6)
La Salle	14,890	13,171	8.7	7.7	(1.0)
Lafayette	221,578	361,856	317.8	519.0	201.2
Lafourche	96,318	112,609	25.3	29.6	4.3
Lincoln	46,735	54,630	38.2	44.6	6.5
Livingston	128,026	314,726	71.5	175.7	104.3
Madison	12,093	8,268	7.2	4.9	(2.3)
Morehouse	27,979	19,510	13.4	9.3	(4.1)
Natchitoches	39,566	37,548	11.8	11.2	(0.6)
Orleans	343,829	310,135	379.5	342.3	(37.2)

Ouachita	153,720	167,523	93.9	102.4	8.4
Plaquemines	23,042	21,107	3.5	3.2	(0.3)
Pointe Coupee	22,802	20,338	14.9	13.3	(1.6)
Rapides	131,613	125,227	37.3	35.5	(1.8)
Red River	9,091	7,174	8.7	6.9	(1.8)
Richland	20,725	18,611	14.2	12.7	(1.4)
Sabine	24,233	22,705	9.2	8.7	(0.6)
St. Bernard	35,897	59,835	6.4	10.7	4.3
St. Charles	52,780	74,669	51.3	72.6	21.3
St. Helena	11,203	11,570	10.6	10.9	0.3
St. James	22,102	21,233	33.1	31.8	(1.3)
St. John the Baptist	45,924	60,827	43.3	57.3	14.0
St. Landry	83,384	80,465	34.3	33.1	(1.2)
St. Martin	52,160	68,297	24.7	32.3	7.6
St. Mary	54,650	41,198	18.8	14.2	(4.6)
St. Tammany	233,740	555,517	82.4	195.8	113.4
Tangipahoa	121,097	204,995	55.4	93.8	38.4
Tensas	5,252	2,529	3.2	1.5	(1.6)
Terrebonne	111,860	129,437	20.7	24.0	3.3
Union	22,721	23,720	9.7	10.1	0.4
Vermilion	57,999	70,768	14.5	17.7	3.2
Vernon	52,334	47,403	15.1	13.6	(1.4)
Washington	47,168	48,685	26.9	27.8	0.9
Webster	41,207	35,843	25.9	22.5	(3.4)
West Baton Rouge	23,788	33,301	45.1	63.1	18.0
West Carroll	11,604	9,567	12.4	10.2	(2.2)
West Feliciana	15,625	19,823	14.2	18.0	3.8
Winn	15,313	12,352	6.2	5.0	(1.2)
Louisiana	4,533,372	5,661,868	33.4	41.7	8.3

Appendix D: Historical (1992–2015) Annual Average and 2050-Projected Property Loss, per Capita Property Loss, and per Building Property Loss, by Louisiana Parish (\$2010).

Parish	Annual Property Loss		Annual Per Capita Property Loss		Annual Per Building Property Loss	
	Historical (1992–2015)	Projected (2050)	Historical (1992–2015)	Projected (2050)	Historical (1992–2015)	Projected (2050)
Acadia	3,330	4,531	0.05	0.07	0.13	0.16
Allen	40,186	59,537	1.56	1.95	4.13	5.18
Ascension	45,125	146,601	0.42	0.53	1.11	1.38
Assumption	95	116	0.00	0.01	0.01	0.01
Avoyelles	7,718	9,344	0.18	0.23	0.43	0.54
Beauregard	75,366	119,506	2.11	2.64	5.01	6.28
Bienville	8,127	8,154	0.57	0.71	1.05	1.35
Bossier	86,676	170,150	0.74	0.93	1.76	2.20
Caddo	203,036	237,777	0.80	1.00	1.81	2.27
Calcasieu	150,068	227,269	0.78	0.97	1.83	2.29
Caldwell	5,183	5,923	0.51	0.64	1.04	1.31
Cameron	6,678	6,434	0.98	1.22	1.86	2.38
Catahoula	2,490	2,311	0.24	0.30	0.51	0.65
Claiborne	10,635	11,978	0.62	0.77	1.37	1.73
Concordia	2,300	2,372	0.11	0.14	0.25	0.31
De Soto	12,567	16,856	0.47	0.59	1.02	1.28
East Baton Rouge	181,900	271,983	0.41	0.52	0.97	1.21
East Carroll	439	313	0.06	0.07	0.15	0.19
East Feliciana	18,926	23,453	0.93	1.17	2.36	2.96
Evangeline	20,656	25,776	0.61	0.76	1.41	1.77
Franklin	2,046	2,100	0.10	0.12	0.23	0.28
Grant	18,805	31,288	0.84	1.05	2.12	2.67
Iberia	156	209	0.00	0.00	0.01	0.01
Iberville	806	1,003	0.02	0.03	0.06	0.08
Jackson	10,491	11,901	0.64	0.81	1.37	1.73
Jefferson	59,273	70,131	0.14	0.17	0.31	0.39
Jefferson Davis	7,096	8,606	0.22	0.28	0.53	0.67
La Salle	11,035	12,223	0.74	0.93	1.68	2.15
Lafayette	4,166	8,505	0.02	0.02	0.04	0.06
Lafourche	227	331	0.00	0.00	0.01	0.01
Lincoln	30,976	45,269	0.66	0.83	1.59	1.99
Livingston	183,701	564,408	1.43	1.79	3.66	4.58
Madison	463	395	0.04	0.05	0.10	0.12
Morehouse	9,039	7,884	0.32	0.40	0.73	0.91

Natchitoches	26,919	31,936	0.68	0.85	1.45	1.82
Orleans	129,056	145,573	0.38	0.47	0.68	0.85
Ouachita	65,159	88,753	0.42	0.53	1.01	1.26
Plaquemines	1,746	2,000	0.08	0.09	0.18	0.23
Pointe Coupee	1,418	1,580	0.06	0.08	0.13	0.16
Rapides	152,642	181,654	1.16	1.45	2.74	3.43
Red River	3,716	3,670	0.41	0.51	0.90	1.13
Richland	2,815	3,165	0.14	0.17	0.33	0.41
Sabine	23,772	27,926	0.98	1.23	1.68	2.13
St. Bernard	7,119	14,834	0.20	0.25	0.42	0.53
St. Charles	927	1,639	0.02	0.02	0.05	0.06
St. Helena	28,355	36,557	2.53	3.16	5.51	6.91
St. James	1,245	1,495	0.06	0.07	0.15	0.18
St. John the Baptist	5,370	8,887	0.12	0.15	0.31	0.38
St. Landry	7,569	9,136	0.09	0.11	0.21	0.27
St. Martin	567	927	0.01	0.01	0.03	0.03
St. Mary	25	24	0.00	0.00	0.00	0.00
St. Tammany	890,955	2,646,673	3.81	4.76	9.34	11.68
Tangipahoa	359,699	761,153	2.97	3.71	7.18	8.99
Tensas	1,009	603	0.19	0.24	0.30	0.39
Terrebonne	67	96	0.00	0.00	0.00	0.00
Union	12,120	15,802	0.53	0.67	1.07	1.34
Vermilion	367	559	0.01	0.01	0.01	0.02
Vernon	67,130	76,099	1.28	1.61	3.13	3.93
Washington	113,349	146,112	2.40	3.00	5.39	6.75
Webster	29,302	31,884	0.71	0.89	1.52	1.90
West Baton Rouge	1,410	2,466	0.06	0.07	0.15	0.19
West Carroll	2,204	2,273	0.19	0.24	0.44	0.55
West Feliciana	4,144	6,579	0.27	0.33	0.81	1.05
Winn	9,107	9,215	0.59	0.75	1.26	1.62
Louisiana	3,169,063	6,373,906	0.70	1.13	1.61	2.65

FIGURE CAPTIONS

Figure 1| Wildfire burn probability: **(A)** historical (1992–2015), and **(B)** projection for 2050.

Figure 2| Population density by census block: **(A)** 2010, and **(B)** change in population density from 2010 to 2050.

Figure 3| Estimated annual property loss (\$2010) due to wildfire by census block: **(A)** historical (1992–2015), and **(B)** 2050.

Figure 4| Estimated annual per capita property loss (\$2010) due to wildfire by census block: **(A)** historical (1992–2015), and **(B)** 2050.

Figure 5| Estimated annual per building property loss: **(A)** historical (1992–2015), and **(B)** 2050 by census block in Louisiana (\$2010).